Journal of Korean Association of Crystal Growth
Vol. 9, No. 4 (1999) 396-401

TSSG growth, morphology and properties of potassium lithium niobate (KLN) crystals

Tow-Chong Chong, Xue-Wu Xu, Lian Li, Guang-Yu Zhang, H. Kumagai* and M. Hirano*

Data Storage Institute, 10 Kent Ridge Crescent, Singapore 119260, Singapore
**Research Center, Asahi Glass Co. Ltd., Yokohama-shi 221-8755, Japan*

(Received June 9, 1999)

Abstract In the present paper, potassium lithium niobate (KLN) crystals have been grown along <001>, <100> and <110> directions by the top seeded solution growth (TSSG) method from Li- richer melts with different compositions. The morphologies of KLN crystals grown along different directions have been studied, and the well-developed facets have been unambiguously indexed using X-ray goniometer and stereographic projection analysis. The growth mechanism and defects such as cracks and inclusions were discussed on the basis of observations of facets on the crystal-solution interfaces. The crystal compositions were determined by a chemical analysis method. The structure and lattice constants of KLN crystals were determined and calculated on the basis of XRD data by using TREOR90 and PIRUM programs. The Curie temperature and optical absorption were determined by dielectric constant peak and spectrum measurements, respectively. The blue second harmonic generation (SHG) characteristics of a KLN sample were also investigated using a pulsed dye laser.

1. Introduction

Compact, high-efficient and all solid-state blue lasers with long lifetime have found wide applications in many technical fields such as high-density optical data storage and medical science. With the development of high-power semiconductor diode lasers, the search for nonlinear optical crystals suitable for blue second harmonic generation (SHG) has become one of the most important directions for the development of compact blue lasers.

Potassium lithium niobate (KLN) crystal was discovered as a nonlinear optical material in the late 1960s at the Bell telephone laboratories [1]. In the 1970s, much research work was done concerning KLN phase diagram, crystal structure, property and growth [2-7]. In the 1980s, limited by growth technique, the research progress of KLN was very slow. Only a few papers concerning KLN growth and properties were published with interest mainly focused on its piezoelectric applications [8]. Up to the beginning of the 1990s, the discovery of excellent blue SHG properties of KLN spurred rapidly further research on KLN crystals for nonlinear optical applications [9-15]. As compared with the well-known $KNbO_3$ (KN) crystal, KLN exhibits several advantages. Firstly, an as-grown KLN crystal does not undergo as many structural phase transitions as KN from growth temperature to room temperature, and hence has simple domain structures (positive and negative domains). Secondly, KLN is a negative uniaxial crystal that avoids twinning and presents a simple phase-matching configuration ($o-o \rightarrow e$, type I). Thirdly, it has a low optical loss, good mechanical stability, high optical-damage threshold, large birefringence and the ability to tune the non-critical phase-matching (NCPM) wavelength at room temperature from 790 to 920 nm by changing the Li content of the crystal [9-11]. Recently, researchers from the Philips research laboratories have reported their promising blue SHG results by using a KLN crystal in a monolithic ring resonator [10]. It has been demonstrated that KLN is a suitable material for the frequency doubling of a (Al,Ga)As diode laser at room temperature. KLN is also suitable for blue SHG by conversion of Ti : sapphire laser irradiation [12].

Although many different methods [5, 8, 12, 14, 16] have been applied to the growth of KLN crystals, high-quality KLN with centimeter dimensions can not yet be grown in batches due to cracks, inclusions and compositional inhomogeneity. In the present paper, we grow KLN crystals along <001>, <100> and <110> directions by the top seeded solution growth (TSSG) method from Li-richer melts with different compositions. The morphologies of KLN grown along different directions are investigated. KLN crystals are characterized by means of X-ray diffraction (XRD), chemical

analysis, spectrum and dielectric constant measurements. Some preliminary results on the blue SHG characteristics of KLN are also presented.

2. Experimental procedure

According to the phase diagram of K_2O-Li_2O-Nb_2O_5 ternary system [2], in the Nb- richer region, there is a long and relatively narrow KLN solid solution region with tungsten bronze (TB) structure. The composition of this solid solution along 30 mole% K_2O isopleth is represented by a formula $(K_2O)_{0.3}(Li_2O)_{0.7-x}(Nb_2O_5)_x$ or $K_3Li_{2-y}Nb_{5+y}O_{15+2y}$, where $y = 10x - 5$. The completely filled stoichiometric composition $K_3Li_2Nb_5O_{15}$ ($x = 0.5$) does not exist in this phase region. Only KLN crystals containing 51~55 mole% Nb_2O_5 are ferroelectric with a tetragonal TB- type structure and have desired nonlinear optical properties. The ferroelectric Curie temperature, Tc, decreases from above 550°C to below 400°C as the Nb_2O_5 content increases from 51 mole% to 55 mole% [2]. Moreover, these KLN crystals should be grown from melts with the Nb_2O_5 content much lower than 50 mole% due to their incongrugruently melting behavior.

We grew KLN crystals from different melts with the content of Nb_2O_5 in the range 43 mole% to 46 mole% by the TSSG method. The K_2O content of the melt is around 30 mole%. Raw materials were prepared from high purity Nb_2O_5 (4N), Li_2CO_3 (5N) and K_2CO_3 (3N) powders and thoroughly mixed on a ball-milling station (without balls) for 24 h. The mixed components were sintered in the Pt crucible at 850~900°C for 4~6 h before melting. Typical growth parameters are: pulling rate 0.1~1 mm/h, rotation rate 8~20 rpm, growth temperature ~1000°C, cooling rate for growth 0.1~0.5°C/h, Pt crucible size 60 mm diameter and 75 mm height. The growth directions are <001>, <100> and <110>, respectively.

The crystal morphology was investigated using a Rigaku X-ray goniometer and stereographic projection analysis. X-ray diffraction (XRD) measurements were conducted on a Philips APD 1700 diffractometer using Ni filtered Cu Kα radiation in the range of $2\theta = 20°$ to 80°. Crystal compositions were measured by chemical analysis. The dielectric constants, ε_{33}, were measured with a LCR meter HP 4284A from room temperature to 600°C at 1 and 10 kHz, respectively. A sample for spectral measurement was cut perpendicularly to the <001> axis. Its two parallel {001} planes were then lapped and polished to a thickness of 0.48 mm. The transmittance and reflectance (for 5° incidence angle) were measured at room temperature with a Shimadzu UV-VIS-NIR scanning spectrophotometer model UV-3101PC. The blue SHG characteristics of the KLN crystals were measured by using a Continuum ND 6000 dye laser with ~30 ns pulse width, 10 Hz repetition rate and 820~907 nm wavelength range, which was pumped by the second harmonic wave of a pulsed Nd : YAG laser operating at 1064 nm. A (001)-cut KLN sample poled by a field-cooling method was fixed on a controlled hot stage (20~60°C), with the incidental fundamental beam perpendicular to the <001> axis, enabling the type I NCPM configuration to be realized.

3. Results and discussion

3.1. Crystal growth and morphology

The growth of KLN crystals has shown a strong anisotropic habit. The <001> grown KLN has a square cross-section dominated by four {110} facets, which were determined by an X-ray goniometer. Smaller {210} facets with an included angle of 126.9° can be seen at the corners of the square (Fig. 1a). Other crystal planes with lower index such as {100} and {310} did not occur (refer to Fig. 1b). Such crystal morphology is different from that observed by previous researchers [8], where {100} facets were observed. The crystals abruptly withdrawn from the melt usually showed a flat interface dominated by {001} facets. Crack-free columnar KLN with size up to $4\times4\times50\ mm^3$ could be grown along <001> axis. However, with the increase of crystal diameter, many crystals showed cracks and visible inclusions, especially near the bases, where the interfaces became partially faceted and cellular growth was observed. The <100> grown KLN usually has a rectangular cross-section with longer edges parallel to <001> and relatively shorter edges parallel to <010>. The crystal-melt interfaces of these crystals are greatly convex to the melt and bounded by {110}, {210} and {100} facets (see Fig. 2a). Figure 2b gives a (100) stereographic projection of the KLN tetragonal system. The <110> grown KLN also shows a rectangular cross-section with longer edges parallel to <001> and much shorter edges parallel to $<1\bar{1}0>$, which suggested that the growth rate along <001> is much larger than that along <110>. Viewed along the <001> direction, a

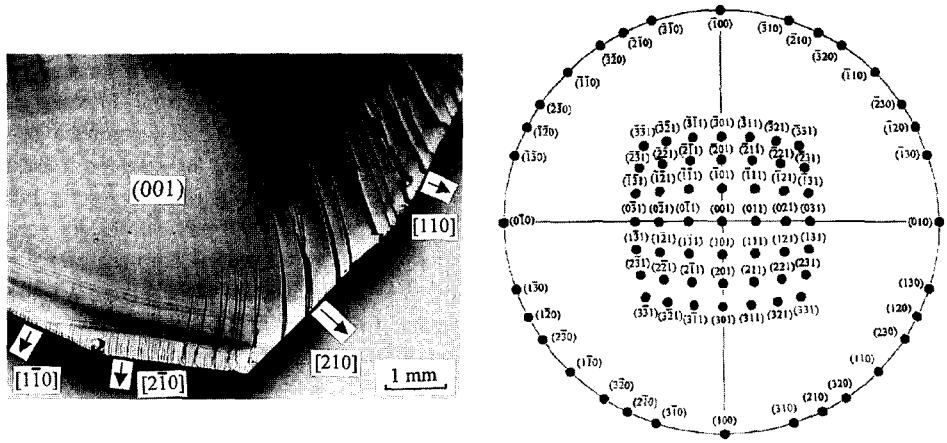

(a) (b)

Fig. 1. (a) A corner of the square cross-section of a [001] grown KLN crystal; (b) (001) stereographic projection of the KLN tetragonal system.

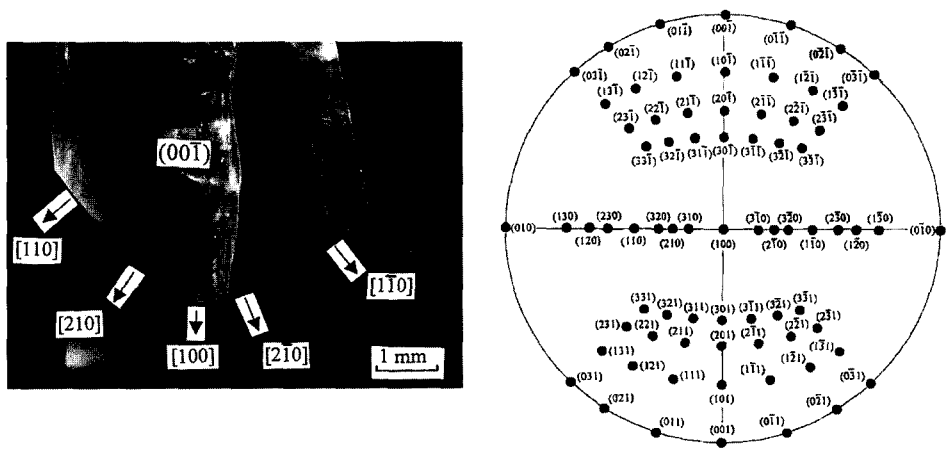

(a) (b)

Fig. 2. (a) Crystal-melt interface for the [$\bar{1}$00] growth, viewed along [001]; (b) (100) stereographic projection of the KLN tetragonal system.

series of {001} growth terraces could be clearly observed on the expanding shoulder of the <110> grown KLN. However, the growth interfaces of these crystals are slightly convex to the melt and bounded by one larger flat {110} facet and two relatively smaller {210} facets (Fig. 3a). These long and narrow facets are well developed and parallel to <001> (Fig. 3b). According to the above observations, the most predominant face that appears in the KLN growth form should be {110}, followed by {210}, {001} and {100}. Figure 4 shows some KLN crystals grown along different axes. We noticed that transparent and inclusion-free KLN crystals with centimeter size could be obtained by growing along <100> or <110> axes although some cracks mainly parallel to the {001} cleavage plane existed in these crystals. This may be ascribed to the differences in growth mechanism caused by different facet morphologies on the crystal-melt interfaces. The interfaces completely bounded by the {110} and {210} facets with slower growth rate make the <100> and <110> growth stable as compared with the <001> growth, where the interface of <001> grown crystal of large diameter was usually convex to the melt and partially faceted.

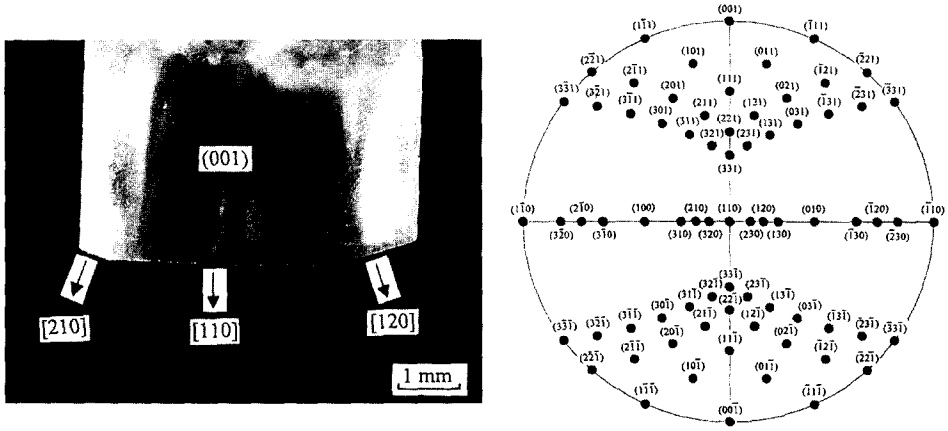

Fig. 3. (a) Crystal-melt interface for the [110] growth, viewed along [00$\bar{1}$]; (b) (110) stereographic projection of the KLN tetragonal system.

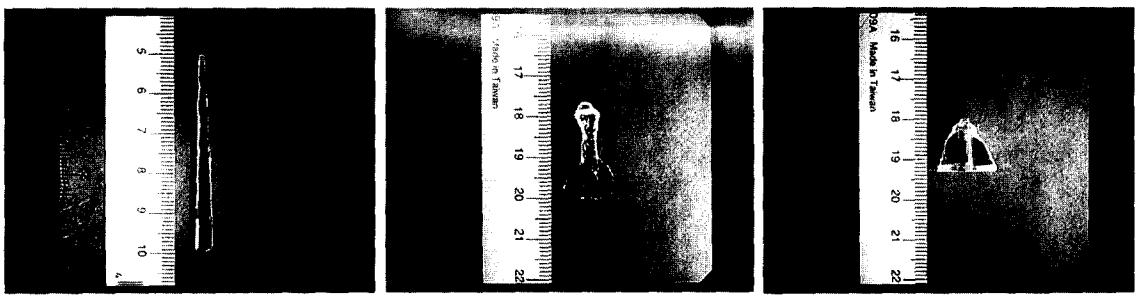

Fig. 4. Some KLN crystals grown along (a) <001>, (b) <100> and (c) <110>.

3.2. Crystal composition and structure

KLN crystal compositions were measured by the chemical analysis method. Table 1 gives the melt compositions used in our growth experiments and their corresponding crystal compositions (except for KLN5). The large difference between the crystal and melt compositions indicates that the KLN crystals are incongruently-melting solid solutions. In these cases, the effective segregation coefficient of K_2O is near unity (0.85~0.98). The coefficient of Li_2O is much less than the unity (0.70~0.80). While the coefficient of Nb_2O_5 is much more than the unity (1.16~1.21). Such non-unity segregation, especially for Li and Nb around 30 mole% K_2O isopleth will cause melt compositional changes with the withdrawal of growing crystals and finally the crystal compositional inhomogeneity along growth directions.

The XRD analysis of crystal powders confirmed that the KLN crystals have a tetragonal TB-type structure. The trial-and-error indexing program, TREOR90 [17], was first used for indexing and determination of cell parameters. The cell parameters obtained with the TREOR90 program were then refined with the pro-

Table 1
Compositions of melts and crystals

Sample No.	Melt composition (mole %)			Crystal composition (mole %)		
	K_2O	Li_2O	Nb_2O_5	K_2O	Li_2O	Nb_2O_5
KLN1	30.0	27.0	43.0	28.1	19.8	52.1
KLN2	30.5	26.5	43.0	29.4	19.4	51.2
KLN3	29.5	27.5	43.0	28.9	19.2	51.9
KLN4	30.0	26.0	44.0	29.2	19.5	51.2
KLN5	30.0	25.0	45.0	-	-	-
KLN6	31.0	24.0	45.0	28.4	18.6	53.0
KLN7	33.0	22.0	45.0	28.3	17.7	54.0
KLN8	30.0	24.0	46.0	28.7	17.8	53.5

gram PIRUM [18]. All the reflection lines based on the XRD data could be indexed in a tetragonal system. For the crystal KLN1, the results of this analysis gave a = b = 12.565±0.002 Å and c = 4.034±0.001 Å with figure of merit $M_{(20)}$ = 24 and $F_{(20)}$ = 32. While for the crystal KLN8, the results gave a = b = 12.5693±0.0005 Å and c = 4.0115±0.0003 Å with $M_{(20)}$ = 46 and $F_{(20)}$ = 61. We can see that the axial ratio $\sqrt{10}c/a$ is larger than 1 and decreases with the increase of Nb_2O_5 content in the crystal, which is in agreement with the results of previous workers on ceramic samples [2].

3.3. *Dielectric constant and Curie temperature*

As mentioned in section 2, the KLN crystals with different Nb_2O_5 content will have a different ferroelectric Curie temperature. Figure 5 shows the dielectric constant ε_{33} versus temperature of the crystal KLN5 at different frequencies during the heating process. The maxima of the dielectric constant are observed around 485°C and 463°C for 1kHz and 10 kHz, respectively. The broadening of the dielectric constant peak represents the diffuse phase transition of KLN crystal. A larger dielectric constant and a higher temperature at the peak of 1 kHz curve indicates that KLN has larger dielectric relaxation in the lower frequency region [19].

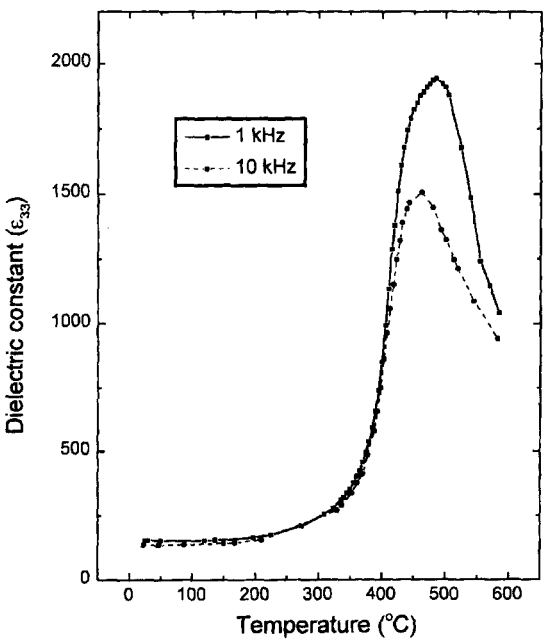

Fig. 5. Dielectric constant ε_{33} versus temperature at 1 kHz and 10 kHz.

3.4. *Transmittance, reflectance and absorption coefficient*

Figure 6 shows the transmittance (T %) and reflectance (R %) of the crystal KLN5 with a thickness of t = 0.048 cm. The transmission limit is about 370 nm. As the reflectance was measured from a double-sided polished sample, the absorption coefficient α could be calculated by using $\alpha t = -\ln\{T/(1-R)\}$ [20]. The decrease of the reflectance near the transmission limit may be ascribed to the absorption of the light reflected by the second polished face. The calculated absorption coefficient is shown in Fig. 7. It is shown that the crystal has very small optical absorption at the wavelength larger than 400 nm, which is favorable for blue SHG applications.

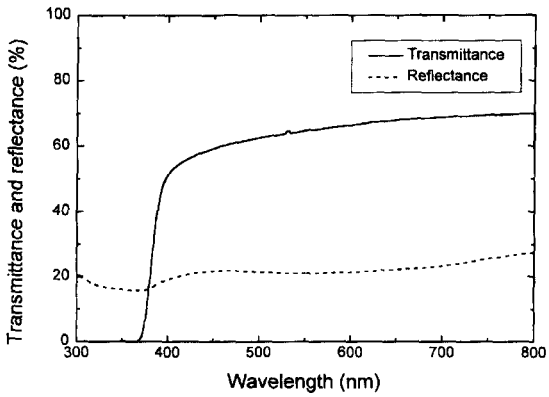

Fig. 6. Transmittance and reflectance of a KLN sample with a thickness of 0.048 cm.

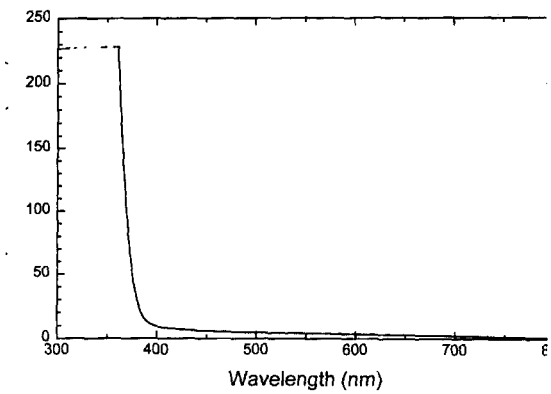

Fig. 7. Absorption coefficient calculated from the data shown in Fig. 6.

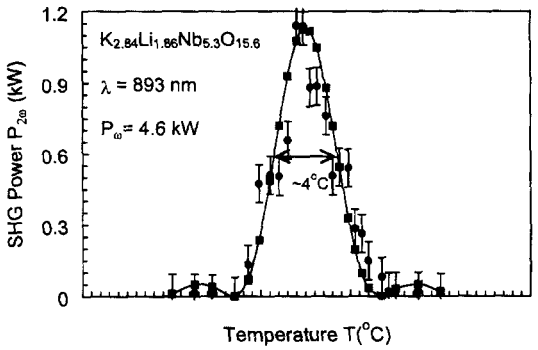

Fig. 8. Dependence of SHG power on temperature

3.5. Blue SHG characteristics

The blue SHG experiments were carried out on a sample taken from the crystal KLN6. By changing the wavelength of the fundamental beam continually, the non-critical phase matching (NCPM) could be realized at $\lambda = 886$ nm with a wavelength acceptance of 1.5 nm. The measurement of the dependence of SHG power on the fundamental beam power showed that a 20 % efficiency could be attained under the pulsed dye laser. With the increase of crystal temperature, the extraordinary refractive index of the KLN crystal increases while the ordinary refractive index remains unchanged [4, 6]. Therefore, the NCPM can also be realized at a longer wavelength by tuning the crystal temperature. Figure 8 gives the dependence of SHG power on temperature, showing a wide temperature acceptance of about 4°C, one order higher than that of KN crystal. More detailed studies on the blue SHG characteristics of the KLN crystals are currently in progress by using a CW tunable Ti : sapphire laser.

4. Conclusions

The KLN crystals have been grown along <001>, <100> and <110> directions by the TSSG method. The Nb_2O_5 content of the melts used for the crystal growth changed from 43 mole% to 46 mole% while the K_2O content varied around 30 mole%. The strong anisotropic growth led to different crystal forms for the growth along different directions. The observed order in morphological importance is {110}, {210}, {001} and {100}. The crystal-melt interfaces for the growth along <100> and <110> are always bounded by {110}, {210} and sometimes {100} crystallographic facets, while the interface for the <001> growth is usually flat and dominated by {001} facets. The crystals grown from different melts have different compositions due to the non-unity segregation effect. The KLN crystals have shown a tetragonal TB-type structure with the axial ratio $\sqrt{10}c/a$ larger than 1 and decreasing with the crystal Nb_2O_5 content. The broadening of the dielectric constant peak around 463°C shows the behavior of diffuse phase transition in the KLN. The transmission limit of about 370 nm and very small absorption coefficient in the visible region make the KLN crystal favorable for blue SHG applications. A high SHG efficiency (20 %), a wide wavelength acceptance (~1.5 nm) and a large temperature acceptance (~4°C) have been demonstrated on a KLN crystal under the pulsed dye laser.

References

[1] L.G. Van Uitert, S.Singh, H.J. Levinstein, J.E. Geusic and W.A. Bonner, Appl. Phys. Lett. 11 (1967) 161.
[2] B.A. Scott, E.A. Giess, B.L. Olson, G. Burns, A.W. Smith and D.F. O'Kane, Mat. Res. Bull. 5 (1970) 47.
[3] S.C. Abrahams, P.B. Jamieson and J.L. Bernstein, J. Chem. Phys. 54 (1971) 2355.
[4] A.W. Smith, G. Burns, B.A. Scott and H.D. Edmonds, J. Appl. Phys. 42 (1971) 684.
[5] F.W. Ainger, J.A. Beswick, W.P. Bickley, R. Clarke and G.V. Smith, Ferroelectrics 2 (1971) 183.
[6] T. Nagai and T. Ikeda, Japan. J. Appl. Phys. 12 (1971) 199.
[7] M. Adachi and A. Kawabata, Japan. J. Appl. Phys. 17 (1978) 1969.
[8] R.R. Neurgaonkar, W.K. Cory, J.R. Oliver and L. Eric Cross, Mat. Res. Bull. 24 (1989) 1025.
[9] M. Ouwerkerk, Adv. Mater. 3 (1991) 399.
[10] J.J.E. Reid, M. Ouwerkerk and L.J.A.M. Beckers, Philips J. Res. 46 (1992) 199.
[11] J.J.E. Reid, Appl. Phys. Lett. 62 (1993) 19.
[12] D.H. Yoon, M. Hashimoto and T. Fukuda, Jpn. J. Appl. Phys. 33 (1994) 3510.
[13] D.H. Yoon, P. Rudolph and T. Fukuda, J. Crystal Growth 144 (1994) 207.
[14] M. Ferriol, G. Foulon, A. Brenier, M.T. Cohen-Adad and G. Boulon, J. Crystal Growth 173 (1997) 226.
[15] Q. Jiang, T.P.J. Han and H.G. Gallagher, J. Mater. Sci.: Materials in Electronics 9 (1998) 193.
[16] T. Fukuda, Japan. J. Appl. Phys. 8 (1969) 122.
[17] P.E. Werner, L. Eriksson and M. Westdahl, J. Appl. Crystallogr. 23 (1990) 292.
[18] P.E. Werner, J. Appl. Cryst. 9 (1976) 216.
[19] B.M. Jin, A.S. Bhalla, B.C. Choi and J.N. Kim, Phys. Stat. Sol. (a) 140 (1993) 239.
[20] V. Srikant and D.R. Clarke, J. Appl. Phys. 83 (1998) 5447.